IEEE Access
Multidisciplinary | Rapid Review | Open Access Journal

Received April 8, 2019, accepted April 30, 2019, date of publication May 10, 2019, date of current version May 21, 2019.

Digital Object Identifier 10.1109/ACCESS.2019.2915925

Data-Driven Control of Ground-Granulated Blast-Furnace Slag Production Based on IOEM-ELM

XIAOLI LI[1,2,3,4], KANG WANG[1,2], AND CHAO JIA[5]

[1]Faculty of Information Technology, Beijing University of Technology, Beijing 100124, China
[2]Beijing Key Laboratory of Computational Intelligence and Intelligent System, Beijing Laboratory for Urban Mass Transit, Beijing 100124, China
[3]Beijing Advanced Innovation Center for Future Internet Technology, Beijing 100124, China
[4]Engineering Research Center of Digital Community, Ministry of Education, Beijing 100124, China
[5]China Electronics Standardization Institute, Beijing 100007, China

Corresponding author: Kang Wang (wangkang@bjut.edu.cn)

This work was supported in part by the National Natural Science Foundation of China under Grant 61873006, Grant 61473034, and Grant 61673053, in part by the Beijing Major Science and Technology Special Projects under Grant Z181100003118012, and in part by the National Key Research and Development Projects under Grant 2018YFC1602704 and Grant 2018YFB1702704.

ABSTRACT An improved online error minimized- extreme learning machine (IOEM-ELM) adaptive control method is proposed by introducing the adding and pruning mechanism of hidden nodes to realize the control of a kind of MIMO system with multiple operating modes. The strategy to handle the multiple-operating-modes problem is analyzed by the idea of multiple model adaptive control. Further, considering that the ground-granulated blast-furnace slag (GGBS) production process is a complex system with the characteristics of multiple operating modes, high nonlinearity, strong coupling, and high uncertainty, a data-driven intelligent control scheme is designed based on the proposed IOEM-ELM neural network. By analyzing the numerous production data produced in normal and abnormal situations, three typical operating modes are extracted to fully depict the actual production process as a testing platform. As the network structure adjusts dynamically using the IOEM-ELM method, model, and controller are designed to deal with the GGBS production process operating among multiple modes. The example shows that the proposed method can handle changing modes, and reduce the computation of GGBS production process effectively.

INDEX TERMS IOEM-ELM, ground-granulated blast-furnace slag, neural network, multiple operating modes, multiple model adaptive control.

I. INTRODUCTION

When dried and ground thinner than 400 m^2/kg, wasted slag produced in the smelting process of the blast furnace turns into a new kind of powder product called ground-granulated blast-furnace slag (shorted as GGBS). As an environmental-friendly material, GGBS can be doped into ordinary Portland cement to improve its mechanical properties significantly [1]. GGBS has been widely used in construction, railway laying and underwater tunnel for its superiority in concrete durability, extending the lifespan of buildings from fifty years to a hundred years. Defined as the total surface area of a material per unit of mass, specific surface area (SSA) indicates the quality of GGBS product. The main production mechanism is the slag's physical change finished in the vertical grinding mill. Mixed with a small amount of grinding aids, wet slag from blast furnace is dried and ground to become GGBS product until it satisfies the SSA requirement. The higher the SSA is, the better the quality will be, and it needs more grinding at the same time. Thus, productivity and SSA reflect the cost and quality of GGBS production directly.

Due to multiple variables and complex unknown physical and chemical changes in mill, GGBS grinding is a strongly nonlinear, coupled and highly uncertain production process, and its mechanism model is hard or impossible to be established precisely. Though the mechanism of GGBS production is deeply researched in [2], [3], accuracy of the mechanical model for grinding process is hardly satisfying. In recent years, with the rapid development of neural network (NN), it has been possible to establish neural network models of the complex nonlinear system with data-driven methods [4]–[6]. On one hand, key points in production

The associate editor coordinating the review of this manuscript and approving it for publication was Bin Xu.

process can be modeled based on neural network through its high identification ability for nonlinear systems. At the same time, massive observation data produced in the practical production process lays a solid foundation for neural network modeling. In this mean, introducing neural network into the GGBS production process should be an effective method. Traditional adaptive control methods show relative satisfying control effectiveness for slow time-varying environment. However, in practical control process, model of plant will change abruptly when some accidents happen such system failure or parameter change. Regular adaptive control can hardly deal with this kind of abrupt changes, resulting in the deterioration of transient response. Taking the 'divide and rule' control strategy, multiple model adaptive control (MMAC) supplies an effective solution for system with multiple operating modes [7]–[9]. Multiple models are firstly established to cover the uncertainty of system, then the most appropriate controller is selected among the controller set based on a switching mechanism.

Traditional feed forward neural networks are slower than required because all their parameters are tuned based on the gradient-based learning algorithms. Aimed at this problem, Huang et al proposed the extreme learning machine (ELM) which can randomly choose the input weights and analytically determine the output weights. Thus, the time to tune weight parameters is greatly reduced [10]. Further, Liang *et al.* proposed the OS-ELM (online sequential ELM) when the training data comes one by one or chunk by chunk rather than be prepared in advance [11]. Based on the OS-ELM algorithm, Li *et al.* designed the identification and adaptive control method for nonlinear dynamic system, multiple model adaptive control scheme was introduced to further improve control quality for system with jumping parameters [12]. However, multiple models and controllers must be designed in advance to cover the uncertainties of system. Introducing the error minimized scheme in EM-ELM (error minimized ELM) [13], Jia *et al.* proposed the OEM-ELM (online error minimized-ELM) which can realize structure dynamic increasing of neural networks and online adaptive control of nonlinear system [9]. Though control quality and robustness are improved and ensured for single-mode system, network size will increase continuously due to the single-way network adjusting strategy if OEM-ELM control is applied to system with multiple operating modes.

Considering the characteristic of multiple operating modes, this paper aims to propose a data-driven control method for GGBS production process based on improved OEM-ELM. The basic idea of the improved OEM-ELM neural network to handle multiple operation modes is to adjust NN structure in both ways of adding and pruning based on the identification error to adapt to environmental change. During structure change process of neural network, every structure can be viewed as a system model, in this sense, IOEM-ELM method can be regarded as a new kind of multiple model adaptive control method with model self-adjusting and self-switching mechanism. Taking full use of massive process data, we try to analyze and extract process data in normal production process and process data in abnormal modes, establish models of different operating modes using recurrent neural network, and construct the GGBS testing platform. Finally, the IOEM-ELM control method is applied to identify and control the multi-mode GGBS production process to show the effectiveness of proposed scheme.

The novelties brought up by this paper compared to existing literatures can be summarized by the following points:

- By introducing the nodes pruning strategy, network structure adjusting in both ways of adding and pruning is constructed in the proposed IOEM-ELM control method, realizing the auto-adjusting of network size according to the complexity of controlled plant.
- Adaptive control of MIMO system with multiple operating modes is realized based on the proposed IOEM-ELM method, the control strategy is analyzed according to the idea of multiple model adaptive control which has been recognized as an effective method to handle system with switching modes.
- Intelligent control of complex GGBS production process with three operating modes is realized based on the IOEM-ELM method, satisfying control quality with less computation is obtained.

The rest of this paper is organized as follows. In the second section, based on technological workflow and operation status, the movement process of particles in vertical mill is analyzed, key control variables and controlled variables are extracted out. Then, considering that the GGBS production process works among multiple operating modes, identification and control strategy based on IOEM-ELM method is proposed. In the fourth section, through analyzing and extracting out operation data in different operation cases, multiple operating modes of GGBS production process is formulated, and the proposed control strategy is applied. The final section concludes this paper.

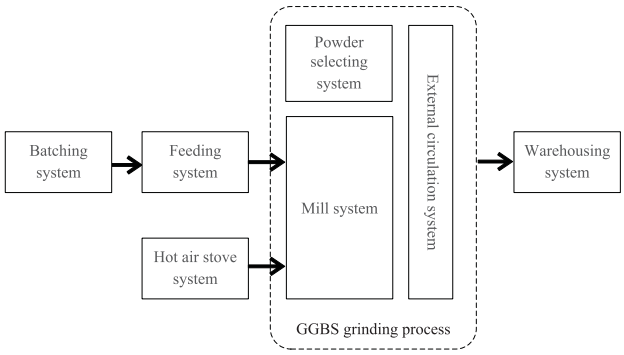

FIGURE 1. Workflow structure of GGBS production.

II. PRODUCTION PROCESS OF GGBS

A. WORKFLOW OF GGBS PRODUCTION PROCESS

GGBS production process consists of batching system, feeding system, hot air stove system, powder selecting system, mill system, external circulation system and warehousing system as shown in Fig. 1. Powder selecting system,

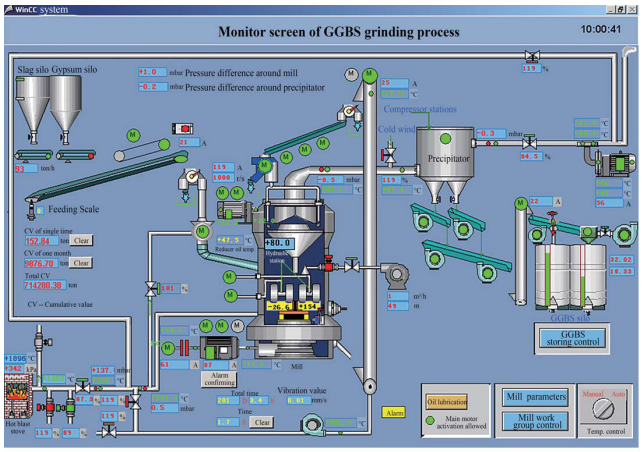

FIGURE 2. Monitor screen of GGBS psroduction.

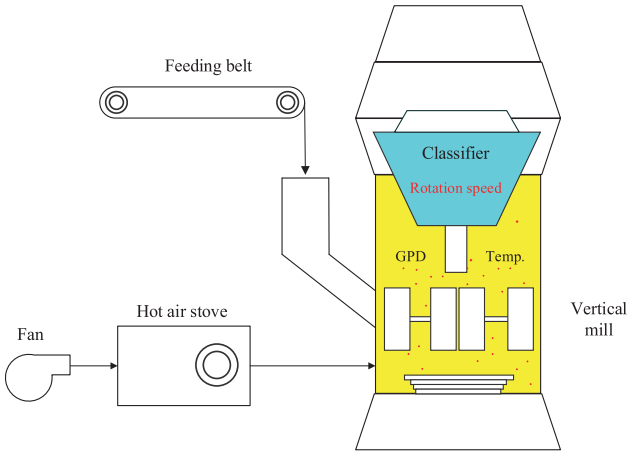

FIGURE 3. Main factors affecting mill vibration.

mill system and the external circulation system compose the GGBS grinding system, which is the key link for GGBS production.

Fig. 2 shows the configuration screen monitoring the production process. Blast furnace slag from the batching equipment is continuously transmitted by feeding belt into the vertical mill for grinding. From bottom to top of the mill, hot wind dries and blows up ground slag powders. Powders up to the selector are selected that those with qualified particle size will be draw out of the mill and taken into the warehouse, those do not satisfy the size requirement will fall into the grinding discs for further grinding. Material with relatively big production size which cannot be taken up by the upstream at the gas ring around the grinding table will fall into the gas channel and be cleared out by the scrapers. Via an encapsulated conveyor and bucket elevator, the reject will be feed into the mill for re-grinding [14].

B. ANALYSIS OF GGBS PRODUCTION PROCESS

The key control target for the grinding system is to guarantee the quality of GGBS production, at the same time, to decrease mill vibration to keep the production process stable. Hence, we start with mill vibration and SSA to analyze the main factors affecting the production process.

1) MILL VIBRATION

Mill vibration is the most dangerous abnormal operation mode for GGBS production. According to the status of GGBS production, mill vibration should be constrained in given range. Once out of this range, it may lead to mill shutting down and even mill blast. In practical production process, there are many factors affecting mill vibration, such as grinding pressure difference (GPD), mill temperature and rotation speed of the classifier as shown in Fig. 3.

Grinding pressure difference denotes the difference between pressure at the lower part of grinding chamber and the pressure at the outlet of hot gas. Lower GPD means relative less feed material and thinner material layer which may cause more contact between the roller and the grinding track bed, leading to strong vibration. Higher GPD means more powders in mill and thicker material layer which may cause mill burst and other extreme hazard events.

Because of the electrostatic interaction, higher mill temperature makes large number of fine particles gather together, fall down and reground. It reduces the grinding effectiveness and may lead to mill vibration. Lower mill temperature affects the quality of final product as it makes the moisture in feed material hard to be evaporated through the heating of hot gas.

Higher rotation speed of the classifier strengthens the selecting process, though quality will be improved, more grinding material falls into the bottom of mill because less material can confirm the size requirement. Consequently, thicker material layer will cause higher GPD and finally leads to mill vibration.

2) SPECIFIC SURFACE AREA

SSA is a key quality index of GGBS product. Higher SSA means finer GGBS powder and better product quality. When the slag is ground finer than 400 m^2/kg, the GGBS powder can be mixed into the cement with a certain proportion, so that mechanical property of the cement concrete will be greatly improved. Further, the product is called super fine GGBS when the slag is ground finer than 500 m^2/kg, which shows stronger activity [15]. There are many factors affecting the SSA of the product.

GGBS is obtained from slag — a by-product of iron and steel-making from blast furnace. Actual production process shows that different kinds of slag from different iron and steel-making blast furnace are different in their hardness and moisture content, which affect the yields and fineness of the GGBS product. In this sense, stability of the material is essential for the stability of the product.

Given certain air speed, higher air volume will blow and take up more material to the classifier, leading to higher product yields but larger particle size, that is, worse product quality. On the other hand, lower air volume will cause finer grain size but lower production yields, more material will

fall back to the grinding table affecting the thickness of the material layer. Thus, the hot air into the mill has great effect on the SSA of the product.

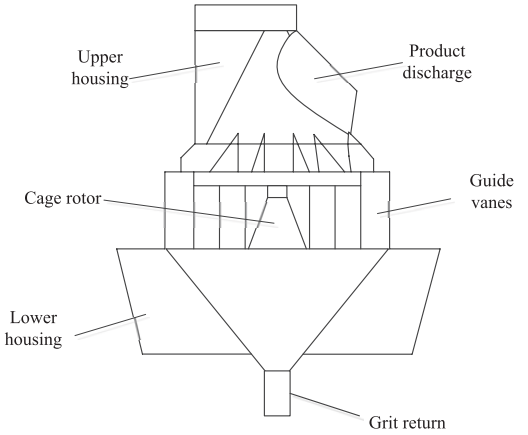

FIGURE 4. Structure diagram of the classifier.

Rotation speed of the classifier have directive effect on the quality of GGBS. Fig. 4 shows the structure diagram of the classifier. Material grading is finished based on two forces acting on particles, the centrifugal force F_c caused by high-speed rotation, and the resistance force F_r by the airflow in the radial direction. When $F_r < F_c$, particles move towards the edge of the classifier and falls into the internal grit return cone and the grinding table for further grinding. When $F_r > F_c$, particles are thin enough to go out of the classifier carried by the airflow and turn into qualified product. When $F_r{=}F_c$, i.e. the centrifugal force equals the resistance force, particles have the same probabilities to come into large powders falling towards the edge, and to come into fine powders carried out of classifier [16]. In practical production process, airflow velocity does not vary much as the outlet airflow volume is required to be stable. Consequently, the rotation speed is the main method to control the fineness of the product. By using the variable frequency speed regulation system, fineness of the product can be controlled continuously.

In summary, the main factors affecting the vibration and SSA of product are GPD, thickness of material layer, material feeding rate, inlet airflow volume, rotation speed of classifier and so on. These factors couple, affect and restrict with each other.

C. DYNAMIC DESCRIPTION OF GGBS GRINDING PROCESS

Through analyzing process workflow of GGBS production system, factors and necessary conditions affecting the product quality and stable operation, the GGBS production process can be described as follow.

Controlled variables: specific surface area S, grinding pressure difference P_d.

Control variables: material feeding rate m, rotation speed of classifier s, temperature of inlet air T, valve opening of inlet cold air p, and other constant parameters θ such as moisture content, airflow volume and inlet airflow pressure.

Dynamic equation of GGBS production process can be described as

$$\dot{x} = f(x, \theta, u) \tag{1}$$

where $x = [x_1, x_2]^{\mathrm{T}}$, $u = [u_1, u_2, u_3, u_4]^{\mathrm{T}}$, $x_1 = S$, $x_2 = P_d$, $u_1 = m$, $u_2 = s$, $u_3 = T$, $u_4 = p$.

As the GGBS production process is multi-variable, highly nonlinear and strongly coupled, traditional model analysis methods based on process mechanism cannot establish precise dynamic functions. On the other hand, GGBS production process generates and storages massive process data at every time instant, which contains valuable information about equipment and operation process. Based on large amount of process data, establishing the data-based model of the plant utilizing neural network, and further designing controller based on neural network can be viewed as an effective control solution for the GGBS production problem.

III. IOEM-ELM BASED ADAPTIVE CONTROL FOR SYSTEM WITH MULTIPLE MODES

Based on the idea of multiple model adaptive control and the characteristic that hidden nodes of OEM-ELM neural network can add dynamically, neural network self-adjusting is introduced to improve OEM-ELM, and the identifier and controller for nonlinear system with multiple operating modes using the improved OEM-ELM neural network are designed.

A. OEM-ELM NEURAL NETWORK

Analyzing corresponding advantages of OS-ELM [12] and EM-ELM [11], paper [9] combines above two methods and proposes the OEM-ELM algorithm. By introducing EM-ELM to evaluate the neural network structure, proposed OEM-ELM can realize the online dynamic adjusting of the NN's structure. Core idea of OEM-ELM is learning segmentally, evaluating NN's performance after every segment, and adding the number of NN nodes spontaneously.

Select the initial training sample set $\aleph_0{=}\{(x_i, t_i)\}_{i=1}^{N_0}$ from given training set $\aleph{=}\{(x_i, t_i)\}_{i=1}^{N}$, $x_i \in \Re^m$, $t_i \in \Re^n$ for initial training of the neural network, where $N_0 < N$. Give activation function $G(a, b, x)$ and initial number of hidden layer nodes $L_0, N_0 \geq L_0$. Initialize the upper limit M_δ for the adding number of hidden nodes every node adjusting time, expected learning accuracy ε, and the number of learning data chunk J at every learning phase. Diagram of OEM-ELM algorithm is given in Fig. 5, from which we can be see that the OEM-ELM algorithm is in two phases, OS-ELM online learning phase and EM-ELM evaluating phase. At each online learning phase, output weights of the NN will learn and adjust online using the OS-ELM algorithm. After learning for J chunks of data, the network output error E will be calculated and compared with the accuracy requirement, if $E \leq \varepsilon$, node growing procedure completes and new coming data drunk is learned consequently. Otherwise, neural network structure will be adjusted using the EM-ELM algorithm that the hidden nodes will be added until the accuracy requirement is confirmed.

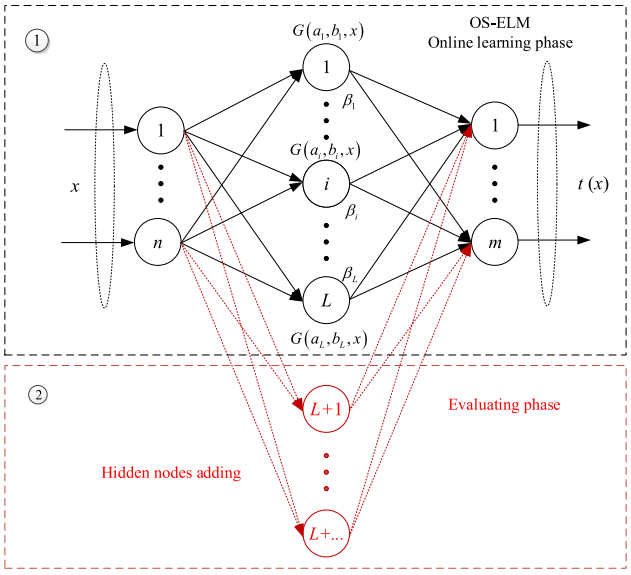

FIGURE 5. Diagram of OEM-ELM NN structure adjusting.

OEM-ELM NN can be viewed as a kind of OS-ELM NN with online NN structure adjusting.

B. PROBLEM FORMULATION

Considering the following discrete-time nonlinear system

$$x_{k+1} = f[x_k] + g[x_k]u_k \tag{2}$$

where $x_k \in \Re^n$ is system output and $u_k \in \Re^m$ is the input. $f \in \Re^n$ and $g \in \Re^{n\times m}$ are piecewise continuous function in the following form

$$\{f, g\} = \begin{cases} \{f_1, g_1\} & k \in [0, k_1] \\ \vdots & \vdots \\ \{f_\tau, g_\tau\} & k \in [k_{\tau-1}, k_\tau] \\ \vdots & \vdots \\ \{f_\hbar, g_\hbar\} & k \in [k_{\hbar-1}, \infty] \end{cases} \tag{3}$$

where $\hbar$ is a finite positive integer, f_τ and g_τ, $\tau \in \{1, 2, \cdots, \hbar\}$ are smooth functions (i.e. infinite differentiable function) with respect to x_k, g_τ is a nonzero bounded function. Assume that f and g do not change frequently, i.e., time interval between two adjacent continuous states is long enough.

For each time interval $[k_{\tau-1}, k_\tau]$ where $\{f, g\}$ is continuous, assume that there exist exact weights w^* and v^*, which guarantee $\hat{f}\left[x_k, w^*\right]$ and $\hat{g}\left[x_k, v^*\right]$ to approximate $f[x_k]$ and $g[x_k]$ precisely. Define w_k, v_k as the estimated values of w^*, v^* at time k, neural network identification model is given in the following form

$$\begin{aligned} \hat{x}_{k+1} &= \hat{f}\left[x_k, w_k\right] + \hat{g}\left[x_k, w_k\right] u_k \\ &= \hat{f}\left[x_k, w_k\right] + \sum_{i=1}^{m} u_{ik}\hat{g}_i\left[x_k, w_k\right] \end{aligned} \tag{4}$$

where $\hat{f}\left[\cdot, \cdot\right]$ and $\hat{g}_i\left[\cdot, \cdot\right]$ are predefined in the following forms of IOEM-ELM neural network

$$\begin{aligned} \hat{f}\left[x_k, w_k\right] &= \sum_{j=1}^{d_1} w_j G(a_j, b_j, x_k), \\ \hat{g}_i\left[x_k, w_k\right] &= \sum_{j=\underline{i}}^{\overline{i}} w_j G(a_j, b_j, x_k) \end{aligned} \tag{5}$$

where

$$\underline{i} = \sum_{l=1}^{i} d_l + 1, \overline{i} = \sum_{l=1}^{i+1} d_l$$

where $a_j \in \Re^n$ and $b_j \in \Re$ are randomly given constant vectors, $j = 1, 2, \cdots, L$, $L = \sum_{l=1}^{m+1} d_l$. Define

$$\begin{aligned} G_i = [&G(a_{\underline{i-1}}, b_{\underline{i-1}}, x_k), G(a_{\underline{i-1}+1}, b_{\underline{i-1}+1}, x_k), \cdots, \\ &G(a_{\overline{i-1}}, b_{\overline{i-1}}, x_k)] \\ \theta_i = [&w_{\underline{i-1}}, w_{\underline{i-1}+1}, \cdots, w_{\overline{i-1}}], i = 1, 2, \cdots, m+1 \end{aligned}$$

Equation (2) can be rewritten as

$$\hat{x}_{k+1} = \Phi_k \hat{\theta}_k \tag{6}$$

where $\Phi_k = [G_1, u_1 G_2, \cdots, u_m G_{m+1}] \in \Re^{n\times L}$, $\hat{\theta}_k = [\theta_1, \theta_2, \cdots, \theta_{m+1}]^{\mathrm{T}} \in \Re^L$.

Model identification error is defined as

$$e^*_{k+1} = x_{k+1} - \hat{x}_{k+1} = x_{k+1} - \Phi_k \hat{\theta}_k \tag{7}$$

C. ADAPTIVE CONTROL BASED ON IOEM-ELM NEURAL NETWORK

According to OEM-ELM algorithm, for every OS-ELM online learning phase, system will execute EM-ELM structure adjusting algorithm once. In the NN adjusting phase, neural network structure will be adjusted (i.e. hidden layer nodes are added based on the EM-ELM algorithm) until the accuracy requirement is confirmed. The main contribution of OEM-ELM is to handle the problem of impropriate initial hidden nodes for fixed plant. Given relative less initial hidden nodes, adaptive control of nonlinear system with fixed operating mode can be achieved by using the nodes adding mechanism, meanwhile, network size will not be too large. However, for system with multiple operation modes described as Equation (2), nodes will add because identification error increases suddenly when modes change occurs, leading to continuously increasing network size no matter the changed mode is more complex or simpler.

In this part, a nodes-pruning strategy is introduced to reduce the hidden nodes when identification error satisfies the minimum accuracy requirement, so that the network structure adjusting can go in both ways of adding and pruning. Workflow of IOEM-ELM adaptive control is depicted in Fig. 6.

For controlled plant with operating modes described as (2), multiple model adaptive control algorithm based on IOEM-ELM is given as follows:

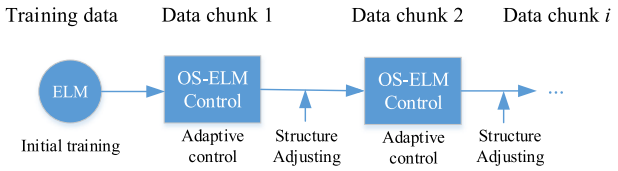

FIGURE 6. Adaptive control based on IOEM-ELM.

1) ADAPTIVE CONTROL ALGORITHM BASED ON IOEM-ELM

Select training data set $\aleph_0 = \{(t_i, o_i)\}_{i=1}^{N_0}$ and initial number of hidden nodes L_0, where $t_i = [x_i; u_i]$, $o_i = x_{i+1}$, $N_0 \geq L_0$. Set the maximum increasing and maximum decreasing numbers of hidden nodes in each adjusting time as M_δ and M_ρ correspondingly. Set the maximum number of hidden nodes L_{M}. Initialize the maximum and minimum identification accuracy ε, ϵ and the number of data chunks J in each learning phase.

Step 1: Initial training

(a) Initialize the hidden nodes parameters $(a_i, b_i), i = 1, \cdots, L_0$ randomly.

(b) Calculate the output matrix of hidden layer Φ_0

$$\Phi_0 = \begin{bmatrix} G(a_1, b_1, x_1) & \cdots & G(a_{L_0}, b_{L_0}, x_1) \\ \vdots & \cdots & \vdots \\ G(a_1, b_1, x_{N_0}) & \cdots & G(a_{L_0}, b_{L_0}, x_{N_0}) \end{bmatrix}_{N_0 \times L_0} \tag{8}$$

(c) Calculate the initial output weight $\theta_0 = P_0 \Phi_0^{\mathrm{T}} T_0$, where $P_0 = (\Phi_0^{\mathrm{T}} \Phi_0)^{-1}$, $T_0 = [t_1, \cdots, t_{N_0}]^{\mathrm{T}}$

(d) Set $k = 1, L = L_0$, go to **Step 2**.

Step 2: IOEM-ELM control

Calculate the output weight

$$\begin{aligned} P_k &= P_{k-1} - \frac{P_{k-1} \Phi_k^{\mathrm{T}} \Phi_k P_{k-1}}{1 + \Phi_k P_{k-1} \Phi_k^{\mathrm{T}}} \\ \hat{\theta}_{k+1} &= \hat{\theta}_k + \sigma_k P_k \Phi_k^{\mathrm{T}} e_{k+1}^* \end{aligned} \tag{9}$$

$0 < \sigma_k < 1$.

Obtain the control signal

$$u_k = \hat{g}[x_k, w_k]^{\dagger} (r_{k+1} - \hat{f}[x_k, w_k]) \tag{10}$$

where r_{k+1} is the expected trajectory, $\hat{g}^{\dagger}$ is the pseudo-inverse matrix of $\hat{g}$.

If $k \geq J$ and $k \% J = 0$, let $j = 1, M_1 = L, \vartheta = \hat{\theta}_{k+1}$, go to **Step 3**.

Step 3: IOEM-ELM structure adjusting

Calculate network error

$$E_j = \left\| Q_j Q_j^{\dagger} Y - Y \right\| \tag{11}$$

where

$$Q_j \triangleq \begin{bmatrix} \Phi_{k-J+1} \\ \vdots \\ \Phi_k \end{bmatrix}_{J \times M_j}$$

$$Y = [x_{k-J+1}, x_{k-J+2}, \cdots, x_k]^{\mathrm{T}}$$

Let the weights of the ith hidden node equal 0, $\vartheta(i, :) = 0$, calculate the significance of the ith node using the root mean squared error.

$$S(i) = \mathrm{RMSE}(Q_j \vartheta - Y) \tag{12}$$

If $M_j < L + M_\delta$ and $E_j > \varepsilon$, then

a: HIDDEN NODES ADDING

$j = j+1$, add δM_{j-1} nodes with the strongest significance into the hidden layer neural network, where δM_{j-1} is a random positive number. The number of hidden nodes becomes $M_j = M_{j-1} + \delta M_{j-1}$, and the output matrix of hidden layer can be written as $Q_j = \left[Q_{j-1}, \delta Q_{j-1}\right]$, where δQ_j is given as Equation (13), as shown at the bottom of this page.

Output weights adjusting law is

$$\begin{aligned} D_j &= \left(\left(I - Q_j Q_j^{\dagger} \right) \delta Q_j \right)^{\dagger} \\ U_j &= Q_j^{\dagger} \left(I - \delta Q_j^{\mathrm{T}} D_j \right) \\ \beta_j &= Q_j^{\dagger} Y = \begin{bmatrix} U_j \\ D_j \end{bmatrix} Y \end{aligned} \tag{14}$$

Let $\vartheta = \beta_j$. Repeat above **Step 3** until $M_j > L + M_\delta$ or $M_j > L_{\mathrm{M}}$ or $E_j \leq \varepsilon$. If $E_j < \epsilon$ and $M_j > L - M_\rho$,

b: HIDDEN NODES PRUNING

Prune ρM_{j-1} nodes with the least significance out of the hidden layer neural network, where ρM_{j-1} is a random positive number. $j = j + 1$. The number of hidden nodes becomes $M_j = M_{j-1} - \rho M_{j-1}$, and the output matrix of hidden layer can be written as $Q_j = \left[Q_{j-1}, \rightharpoonup \rho Q_{j-1}\right]$, where $\rightharpoonup \rho Q_j$ means removing the output matrix of the pruned nodes.

Output weights adjusting law is

$$\beta_j = Q_j^{\dagger} Y = (Q_j^{\mathrm{T}} Q_j)^{-1} Q_j Y \tag{15}$$

Let $\vartheta = \beta_j$. Repeat **Step 3** until $M_j < L - M_\rho$ or $\epsilon \leq E_j \leq \varepsilon$.

Let $L = M_j$, $\hat{\theta}_k = \beta_j$, $k = k + 1$, go to **Step 2**.

Theorem 1: For system with multiple operating modes described as (2), if the IOEM-ELM algorithm is applied, we have

$$\lim_{k \to \infty} \sigma_k \left[\frac{e_{k+1}^2}{\left(1 + \Phi_k P_{k-1} \Phi_k^{\mathrm{T}}\right)^2} - \varepsilon_c^2 \right] = 0 \tag{16}$$

$$\delta Q_j = \begin{bmatrix} G\left(\alpha_{M_{j-1}+1}, b_{M_{j-1}+1}, x_1\right) & \cdots & G\left(\alpha_{M_j}, b_{M_j}, x_1\right) \\ \vdots & \ddots & \vdots \\ G\left(\alpha_{M_{j-1}+1}, b_{M_{j-1}+1}, x_J\right) & \cdots & G\left(\alpha_{M_j}, b_{M_j}, x_J\right) \end{bmatrix}_{J \times \delta M_{j-1}} \tag{13}$$

where control error is defined as $e_k = x_k - r_k$, ε_c is a small constant which represents the upper bound of model error.

Remark 1: In the NN structure adjusting phase, the online error minimized strategy ensures that the NN structure continues adjusting until the neural network can depict current system precisely, and there is no control process. So, it becomes the OS-ELM neural network adaptive control with fixed number of hidden nodes. Thus, stability analysis of IOME-ELM adaptive control for system with constant dynamic can be simplified as the OS-ELM control of system with fixed working mode which can refer to paper [12].

Remark 2: For controlled plant with changing operating modes as (2), because each mode lasts for a relative long time, during each time interval of constant operating mode, proposed algorithm can be viewed as the IOEM-ELM adaptive control for traditional constant controlled plant. When operating mode changes, big overshoot takes place because of the mismatch between neural model and the new operating mode. However, convergence can be guaranteed for the long-time constant mode, and the computation is reduced based to the self-tuning mechanism.

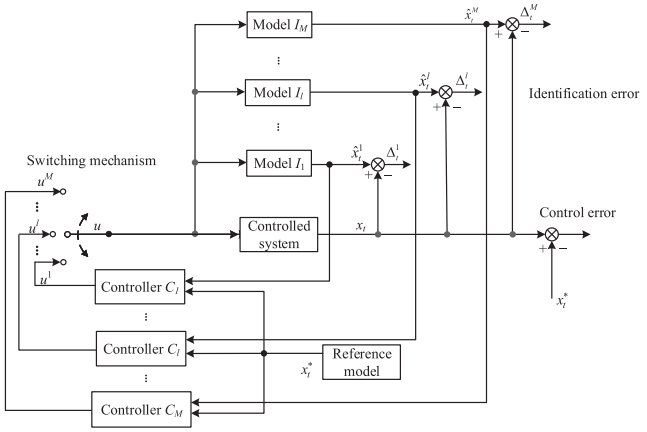

FIGURE 7. Structure of multiple model adaptive control.

Remark 3: Structure of traditional multiple model adaptive control is shown as in Fig. 7. Multiple models are constructed as the model set to cover system's uncertainty. Then, multiple controllers based on corresponding models are designed. Further, an effective switching mechanism is given based on identification error. When model parameters of controlled plant change abruptly, system can detect the change, select and switch to the model closest to current system based on the switching function, and corresponding controller will be switched to control current system. This kind of control strategy can greatly improve transient response of system, solve the big overshot and even uncontrollable problem caused by system parameters abrupt change, guarantee the transition response between different system parameters, and improve the control performance.

Traditional MMAC always focuses on the construct of different models, such as model type (fixed model or adaptive model) [7], [8] and number of models [17], [18], but

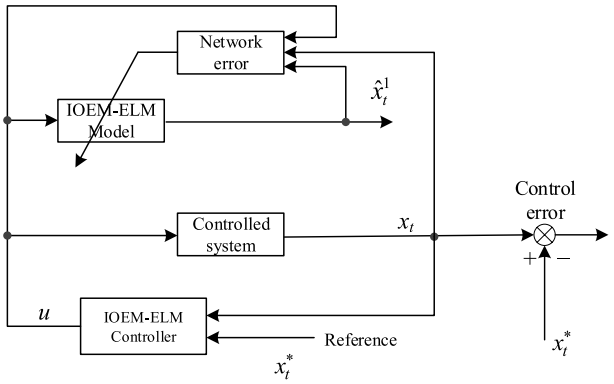

FIGURE 8. Structure diagram of IOEM-ELM adaptive control.

the inner structure of these models will not change in the adaptive progress. The proposed IOEM-ELM NN adaptive controller as shown in Fig. 8 focuses on the inner structure change of model. In the whole identification process, neural network structure will change continuously to adapt to the change of external circumstance. In the NN structure change process, every structure can be viewed as a new model, and the structure adjusting process can be viewed as the model switching process. Thus, IOEM-ELM can be classified as a new multiple model adaptive control pattern in the structure dimension.

IV. ADAPTIVE CONTROL OF GGBS PRODUCTION PROCESS BASED ON IOEM-ELM

Before simulation, we analyze massive production process data, and extract corresponding data sets when production process is normal, and in cases that feed material or rotation speed of classifier is abnormal, to construct the basic frame of multiple operating modes of GGBS production process. Then IOEM-ELM adaptive control is applied to the GGBS production system with multiple changing operating modes.

A. CONSTRUCTION OF EXPERIMENTAL PLATFORM BASED ON RNN

As the main production equipment, vertical mill is a closed container where complex physical and chemical changes happen. Any inappropriate indexes like thickness of material layer or grinding pressure difference may cause the mill to vibrate, leading to operation stop or the danger of explosion. In actual control process, the operator adjusts parameters carefully according to the index in a relatively small area to guarantee an absolute safe operation. The proposed IOEM-ELM algorithm can realize the adaptive control of system with multiple operating modes, however, to guarantee the production process safe, we build the experimental platform to test the control result first before IOEM-ELM is applied to real GGBS production process. In this part, using the recurrent neural network (RNN) to identify the dynamics between control and controlled variables, we construct a testing environment which can describe the real GGBS production process precisely.

Suppose the GGBS production process (1) can be described as

$$\dot{x}_t = A^{*\mathrm{T}} x_t + B^{*\mathrm{T}} F(x_t) + C^{*\mathrm{T}} u_t + D^{*\mathrm{T}} + \varepsilon_t \tag{17}$$

where $x_t \in \Re^n$, $u_t \in \Re^m$, A^*, B^*, C^* and D^* are unknown ideal weight matrix. ε_t is bounded model error. In this paper, activation function $F(x) = \tanh(x)$. According to paper [19], [20], the following dynamic neural network model can be constructed,

$$\dot{\hat{x}}_t = \hat{A}^{\mathrm{T}} \hat{x}_t + \hat{B}^{\mathrm{T}} F(\hat{x}_t) + \hat{C}^{\mathrm{T}} u_t + \hat{D}^{\mathrm{T}} + \upsilon_t \tag{18}$$

where υ_t is defined as

$$\upsilon_t = \Lambda_0 e_t + \frac{\hat{\lambda}_t e_t}{e_t^{\mathrm{T}} e_t + \eta}$$

Identification weights are given as

$$\begin{aligned}
\dot{\hat{A}}_t &= \Lambda_1 \hat{x}_t e_t^{\mathrm{T}} \\
\dot{\hat{B}}_t &= \Lambda_2 F(\hat{x}_t) e_t^{\mathrm{T}} \\
\dot{\hat{C}}_t &= \Lambda_3 u(t) e_t^{\mathrm{T}} \\
\dot{\hat{D}}_t &= \Lambda_4 e_t^{\mathrm{T}} \\
\dot{\hat{\lambda}}_t &= -\Lambda_5 \frac{e_t^{\mathrm{T}} e_t}{e_t^{\mathrm{T}} e_t + \eta}
\end{aligned}$$

where $e_t{=}x_t - \hat{x}_t$ is the model identification error, $\Lambda_i, i = 0, 1, \cdots, 5$ are positive definite matrix with corresponding dimensions. When $t \to \infty$, then $\hat{A} \to A$, $\hat{B} \to B$, $\hat{C} \to C$, $\hat{D} \to D$. Thus, the GGBS production process can be modeled as

$$\dot{x}_t = A^{\mathrm{T}} x_t + B^{\mathrm{T}} F(x_t) + C^{\mathrm{T}} u_t + D^{\mathrm{T}} \tag{19}$$

Through analyzing massive data obtained from GGBS production process as shown in Fig. 9, we extract the most concerned variables in the production process, SSA, GPD, rotation speed of classifier, inlet airflow temperature, valve opening of inlet cold air and so on. After further filtering, we obtain the process data when system is in normal operating mode as shown in Table 1.

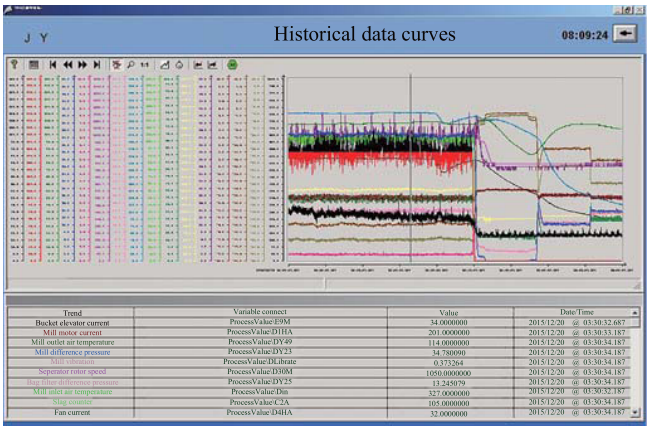

FIGURE 9. Monitoring data of GGBS production system.

When operating mode changes, to verify that the self-organizing IOEM-ELM neural network can adapt to system parameter change by adjusting the number of hidden nodes, we select some data in abnormal operating modes (noted as mode 2 and mode 3) based on massive process data and the experience of engineers to restore the real complex and changeable production process comprehensively. Operating mode 2 shows that the feed material is affected by multiple complex factors so that it is far away from the feed material in normal mode. Mode 3 reflects the mode that the rotation speed of the classifier is far away from the speed in normal state. Table 2 and Table 3 list corresponding process data during some time period in these two abnormal modes.

So far, process data in normal mode, and process data in modes when feed material or rotation speed of classifier

TABLE 1. Process data of GGBS production in operating mode 1.

No.	Feeding rate (10^3kg/Hr)	Rotor speed (r/min)	Mill inlet air temp. (°C)	Circulating air damper opening (%)	SSA (m^2/kg)	GPD (mbar)
1	99.03	1100	228	63.53	439.0	25.5
2	101.09	1100	223	60.55	429.1	26.00
3	103.20	1050	238	60.82	423.9	25.00
⋮	⋮	⋮	⋮	⋮	⋮	⋮
398	100.63	1049	242	60.59	438.5	24.65
399	100.42	1050	243	60.53	426.3	24.94
400	101.20	1051	248	60.62	433.9	25.00

TABLE 2. Process data of GGBS production in operating mode 2.

No.	Feeding rate (10^3kg/Hr)	Rotor speed (r/min)	Mill inlet air temp. (°C)	Circulating air damper opening (%)	SSA (m^2/kg)	GPD (mbar)
1	85.60	1250	230	65.13	440.5	27.60
2	84.81	1160	229	69.50	436.1	28.13
3	84.77	1240	230	66.17	430.7	26.97
⋮	⋮	⋮	⋮	⋮	⋮	⋮
198	85.56	1150	231	66.33	438.5	27.60
199	86.91	1140	233	66.10	426.3	28.13
200	87.77	1140	235	66.17	430.7	26.97

TABLE 3. Process data of GGBS production in operating mode 3.

No.	Feeding rate (10^3kg/Hr)	Rotor speed (r/min)	Mill inlet air temp. (°C)	Circulating air damper opening (%)	SSA (m^2/kg)	GPD (mbar)
1	80.67	698	216	71.10	418.5	26
2	84.81	730	229	69.50	416.3	27.73
3	84.77	760	235	66.17	410.7	27.07
⋮	⋮	⋮	⋮	⋮	⋮	⋮
198	99.63	845	220	72.22	419.1	25.65
199	96.71	898	218	71.89	426.6	25.94
200	96.71	906	229	70.01	483.9	26.00

is abnormal are extracted. On the other hand, three kinds of process data can describe the data state for GGBS production process operating in different operating modes to a large extent. Using massive above data in different operating modes, identification models can be obtained in the RNN form as

$$\begin{aligned} M_1: &\quad \dot{x}_t = A_1^{\mathrm{T}} x_t + B_1^{\mathrm{T}} F(x_t) + C_1^{\mathrm{T}} u_t + D_1^{\mathrm{T}} \\ M_2: &\quad \dot{x}_t = A_2^{\mathrm{T}} x_t + B_2^{\mathrm{T}} F(x_t) + C_2^{\mathrm{T}} u_t + D_2^{\mathrm{T}} \\ M_3: &\quad \dot{x}_t = A_3^{\mathrm{T}} x_t + B_3^{\mathrm{T}} F(x_t) + C_3^{\mathrm{T}} u_t + D_3^{\mathrm{T}} \end{aligned} \tag{20}$$

Select the time interval as $\tau = 0.2$, above continuous functions can be discretized and transformed in the following affine form

$$\begin{aligned} M_1: &\quad x(k+1) = f_1(x(k)) + g_1(x(k))u(k) \\ M_2: &\quad x(k+1) = f_2(x(k)) + g_2(x(k))u(k) \\ M_3: &\quad x(k+1) = f_3(x(k)) + g_3(x(k))u(k) \end{aligned} \tag{21}$$

where f_1, g_1, f_2, g_2, f_3, and g_3 are given in (22), as shown at the bottom of this page.

Without loss of generality, the following multi-modes GGBS production process is considered.

$$x(k+1) = \begin{cases} \text{Mode 1} & k \in [0, 200) \\ \text{Mode 2} & k \in [200, 400) \\ \text{Mode 3} & k \in [400, 600) \\ \text{Mode 2} & k \in [600, 800) \\ \text{Mode 1} & k \in [800, 1000) \end{cases} \tag{23}$$

In the following, adaptive control based on IOEM-ELM algorithm will be applied.

B. IOEM-ELM ADAPTIVE CONTROL FOR GGBS PRODUCTION PROCESS

Select $y = x_1$ as the system output. Desired SSA trajectory after normalization is given as

$$r(k) = 0.755 \; k \in [0, 1000) \tag{24}$$

Initial state is $x(0) = \begin{bmatrix} 0 & 0 \end{bmatrix}^{\mathrm{T}}$.

Construct the IOEM-ELM identification model with the following initial parameters:

Initial number of hidden nodes, $L_0 = 20$

Initial number of learning samples, $N_0 = 200$

Maximum learning accuracy, $\varepsilon = 1 \times 10^{-3}$

Minimum learning accuracy, $\epsilon = 1 \times 10^{-6}$

Upper number limit of adding nodes every adjusting time, $M_\delta = 20$

Upper number limit of pruning nodes every adjusting time, $M_\rho = 2$

Maximum number of hidden nodes $L_{\mathrm{M}} = 100$

Time interval between two network evaluations: $J = 25$

Number of adding and pruning hidden nodes every tuning time, $\delta M = 1$ and $\rho M = 1$

Number of data every data chunk, $N_{k+1} \equiv 1$

For IOEM-ELM neural network, 200 groups of data from mode 1 are selected for initial training with initial parameters set as above. From the identification result in Fig. 10,

$$\begin{aligned} f_1(x(k)) &= \begin{bmatrix} 0.95488x_1(k) + 0.00366x_2(k) + 0.07576\tanh(x_1(k)) + 0.04732\tanh(x_2(k)) + 0.13252 \\ 0.04536x_1(k) + 0.91388x_2(k) - 0.00396\tanh(x_1(k)) - 0.00474\tanh(x_2(k)) + 0.07876 \end{bmatrix} \\ g_1(x(k)) &= \begin{bmatrix} -0.10764 & -0.12507 & -0.0533 & -0.11870 \\ -0.03194 & -0.01016 & -0.01868 & -0.13644 \end{bmatrix} \\ f_2(x(k)) &= \begin{bmatrix} 0.92768x_1(k) - 0.00728x_2(k) - 0.03844\tanh(x_1(k)) + 0.04294\tanh(x_2(k)) + 0.10702 \\ 0.01436x_1(k) + 0.97344x_2(k) - 0.02692\tanh(x_1(k)) + 0.06878\tanh(x_2(k)) + 0.06806 \end{bmatrix} \\ g_2(x(k)) &= \begin{bmatrix} -0.0795 & -0.02426 & 0.0014 & -0.06532 \\ -0.08278 & -0.07898 & -0.00998 & -0.0044 \end{bmatrix} \\ f_3(x(k)) &= \begin{bmatrix} 0.97668x_1(k) + 0.01354x_2(k) + 0.02568\tanh(x_1(k)) - 0.0217\tanh(x_2(k)) + 0.15806 \\ 0.03022x_1(k) + 0.9526x_2(k) - 0.05570\tanh(x_1(k)) + 0.02176\tanh(x_2(k)) + 0.10010 \end{bmatrix} \\ g_3(x(k)) &= \begin{bmatrix} -0.15068 & -0.06478 & -0.04026 & -0.12030 \\ -0.01556 & -0.11478 & -0.07738 & -0.17802 \end{bmatrix} \end{aligned} \tag{22}$$

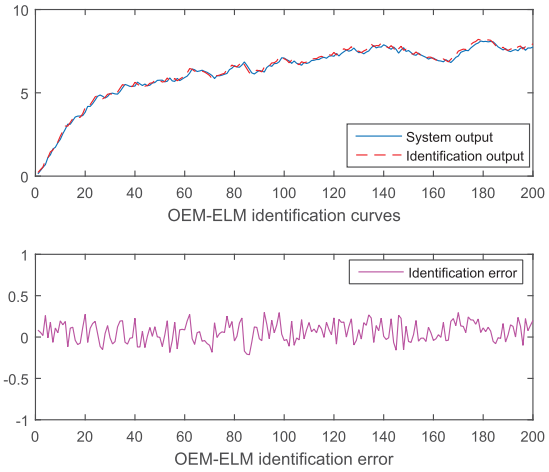

FIGURE 10. Identification result of IOEM-ELM neural network.

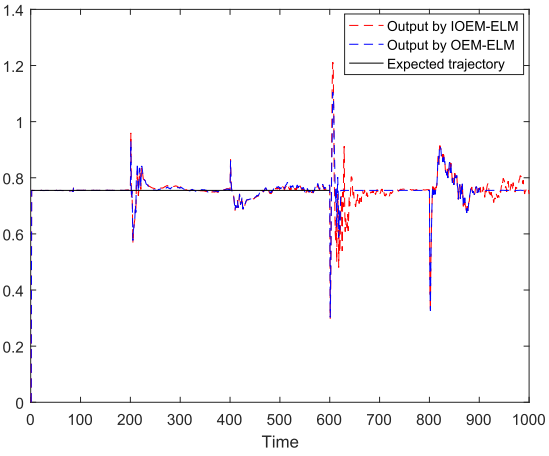

FIGURE 11. Control results by IOEM-ELM and OS-ELM control.

IOEM-ELM neural network can identify the controlled plant effectively, which lays a good foundation for further controller design based on IOEM-ELM. It should be noted that the IOEM-ELM algorithm has two phases, adaptive control based on OS-ELM and structure optimization based on EM-ELM. According to traditional multiple model adaptive control strategy, multiple models and controllers should be established in advance to cover the three operating modes. However, considering that mode change cannot be precisely predicted, switch mechanism of models and controllers cannot be easily determined. Using the IOEM-ELM algorithm, model and controller switch can be finished by adjusting of hidden nodes in neural network. By this means, operating mode change can be timely reflected and good control performance can be obtained.

In this section, IOEM-ELM and traditional OEM-ELM neural network with self-adding scheme are applied, corresponding control results are shown in Fig. 11. Table 4 gives the three indexes–integral absolute error (ISE), integral squared error (ISE) and integral time-weighted absolute error (ITAE) to measure the control performance of both adaptive control methods. Fig. 12 shows the dynamic change of OEM-ELM and IOEM-ELM hidden nodes.

TABLE 4. Performance of IOEM-ELM and OS-ELM adaptive control methods.

Methods	IAE	ISE	ITAE
OEM-ELM adaptive control	3.1957	0.4878	114.4224
IOEM-ELM adaptive control	4.4742	0.6652	202.9861

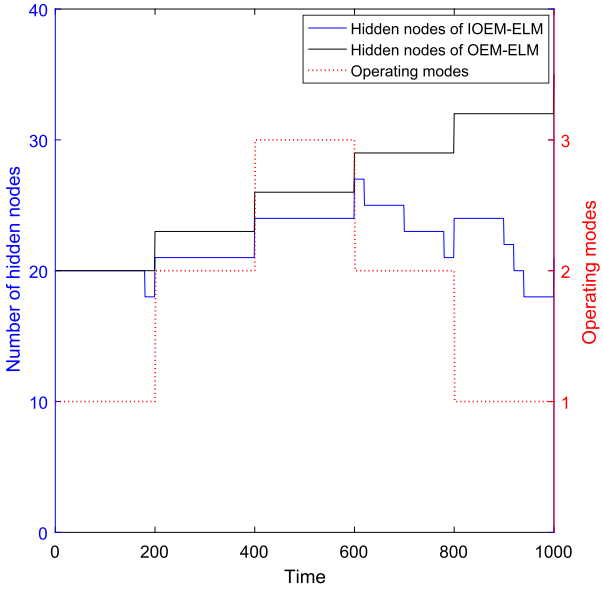

FIGURE 12. Dynamic change of hidden nodes.

From Table 4, it can be seen that the OEM-ELM control algorithm obtains slightly better control performance than IOEM-ELM control in terms of IAE and ISE. The improved control algorithm with less nodes can get satisfying control results. From Fig. 11, we can see that with same initial weights and operating modes, OEM-ELM and IOEM-ELM can both track the desired trajectory. When operating mode change occurs, big overshot takes place in both adaptive control algorithms. However, with the increase of modes changing times, nodes add continuously to get a redundant network in OEM-ELM. This redundancy gets a more accurate identification and faster control result after time 600 compared with the result of IOEM-ELM with less hidden nodes. This result is the same as the ITAE index in Table 4, showing that IOEM-ELM gets a relative slower convergence speed.

Fig. 12 shows the dynamic change of hidden nodes for both IOEM-ELM and OEM-ELM. In the first 200-time intervals, initial 20 hidden nodes satisfy the minimum accuracy requirement for operating mode 1, two redundant nodes are pruned by IOEM-ELM. When modes change occurs at time 200, 400, 600 and 800, identification error increases so that the network structure adjusting mechanism is triggered. Due to lack of nodes pruning strategy, traditional OEM adds nodes continuously from 20 to 32 to reduce the transient error caused by modes change regardless the mode is simple or not. This character causes the network increase continuously as the modes change, leading to the increasing of calculation. While when mode changes from 3 to 2 after time 600, proposed IOEM-ELM adds nodes from 24 to 27 to decease

the identification error in the initial time, and prunes nodes when the minimum accuracy requirement is satisfied. Finally, number of hidden nodes is pruned to 21 which is the same as number for the first mode 2 during time 200 – 400. Same nodes adjusting process runs from time 800 – 1000. In this sense, computation of neural network is greatly reduced compared with traditional OEM-ELM method, especially when modes changing time increases.

V. CONCLUSION

Considering the multi-mode, highly nonlinear, strongly coupled and uncertain characteristics of GGBS production process, a data-driven intelligent control strategy based on IOEM-ELM is proposed. By introducing the hidden nodes pruning strategy, the IOEM-ELM adaptive control method can adjust its network structure in both ways of simplification and complication to adapt to the system change. As a new kind of multiple model adaptive control strategy, IOEM-ELM adaptive control can deal with nonlinear MIMO system with multiple operating modes due to its self-tuning mechanism. Based on massive process data, three typical operating modes are extracted and the changing operating mode is formulated as an experimental platform to describe practical GGBS production process. Then the IOEM-ELM adaptive control method is applied. Simulation shows that the proposed method can deal with abrupt operating mode change effectively and reduce network computation.

REFERENCES

[1] S. A. Miller, P. J. M. Monteiro, C. P. Ostertag, and A. Horvath, "Concrete mixture proportioning for desired strength and reduced global warming potential," *Construct. Building Mater.*, vol. 128, pp. 410–421, Dec. 2016.
[2] L. Duan, X.-L. Li, K. Wang, and Y. Li, "Research on slag grinding process control," in *Proc. 34th Chin. Control Conf. (CCC)*, Hangzhou, China, Jul. 2015, pp. 63–66.
[3] Y. Chen, "Study on separator of large-scale vertical mill," M.S. thesis, Dept. College Mech. Eng., Chongqing Univ., Chongqing, China, 2008.
[4] Y.-J. Liu, S. Tong, C. L. P. Chen, and D.-J. Li, "Neural controller design-based adaptive control for nonlinear MIMO systems with unknown hysteresis inputs," *IEEE Trans. Cybern.*, vol. 46, no. 1, pp. 9–19, Jan. 2016.
[5] Y.-J. Liu, J. Li, S. Tong, and C. L. P. Chen, "Neural network control-based adaptive learning design for nonlinear systems with full-state constraints," *IEEE Trans. Neural Netw. Learn. Syst.*, vol. 27, no. 7, pp. 1562–1571, Jul. 2016.
[6] Y.-J. Liu, S. Tong, D.-J. Li, and Y. Gao, "Fuzzy adaptive control with state observer for a class of nonlinear discrete-time systems with input constraint," *IEEE Trans. Fuzzy Syst.*, vol. 24, no. 5, pp. 1147–1158, Oct. 2015.
[7] X.-L. Li, C. Jia, K. Wang, and J. Wang, "Trajectory tracking of nonlinear system using multiple series-parallel dynamic neural networks," *Neurocomputing*, vol. 168, pp. 1–12, Nov. 2015.
[8] X. L. Li *et al.*, "Nonlinear adaptive control using multiple models and dynamic neural networks," *Neurocomputing*, vol. 136, pp. 190–200, Jul. 2014.
[9] C. Jia, X. L. Li, K. Wang, and D. Ding, "Adaptive control of nonlinear system using online error minimum neural networks," *ISA Trans.*, vol. 65, pp. 125–132, Nov. 2016.
[10] G.-B. Huang, Q.-Y. Zhu, and C.-K. Siew, "Extreme learning machine: Theory and applications," *Neurocomputing*, vol. 70, nos. 1–3, pp. 489–501, 2006.
[11] N.-Y. Liang, G.-B. Huang, P. Saratchandran, and N. Sundararajan, "A fast and accurate online sequential learning algorithm for feedforward networks," *IEEE Trans. Neural Netw.*, vol. 17, no. 6, pp. 1411–1423, Nov. 2006.
[12] X.-L. Li, C. Jia, D.-X. Liu, and D.-W. Ding, "Adaptive control of nonlinear discrete-time systems by using OS-ELM neural networks," *Abstract Appl. Anal.*, vol. 2014, May 2014, Art. no. 267609.
[13] G. Feng, G.-B. Huang, Q. Lin, and R. Gay, "Error minimized extreme learning machine with growth of hidden nodes and incremental learning," *IEEE Trans. Neural Netw.*, vol. 20, no. 8, pp. 1352–1357, Aug. 2009.
[14] Y. Z. Sun, "Vertical roller mill characteristics and its application," M.S. thesis, School Mech. Electron. Eng., Wuhan Univ. Technol., Wuhan, China, 2011.
[15] Y. C. Choi, J. Kim, and S. Choi, "Mercury intrusion porosimetry characterization of micropore structures of high-strength cement pastes incorporating high volume ground granulated blast-furnace slag," *Construct. Building Mater.*, vol. 137, pp. 96–103, Apr. 2017.
[16] S. Z. Liu, J. X. Liu, and L. J. Guo, "Study on theoretical cutting particle size calculation of eddy current air classifier," *Non-Ferrous Mining Metall.*, vol. 22, no. S1, pp. 138–140, 2006.
[17] K. Wang, X. L. Li, and Y. Li, "Multiple model adaptive tracking control based on adaptive dynamic programming," *Discrete Dyn. Nature Soc.*, vol. 2016, Feb. 2016, Art. no. 6023892.
[18] X.-L. Li, D.-X. Liu, C. Jia, and X.-Z. Chen, "Multi-model control of blast furnace burden surface based on fuzzy SVM," *Neurocomputing*, vol. 148, pp. 209–215, Jan. 2015.
[19] Y.-J. Liu, S. Tong, D.-J. Li, and Y. Gao, "Fuzzy adaptive control with state observer for a class of nonlinear discrete-time systems with input constraint," *IEEE Trans. Fuzzy Syst.*, vol. 24, no. 5, pp. 1147–1158, 2016.
[20] H. Zhang, L. Cui, X. Zhang, and Y. Luo, "Data-driven robust approximate optimal tracking control for unknown general nonlinear systems using adaptive dynamic programming method," *IEEE Trans. Neural Netw.*, vol. 22, no. 12, pp. 2226–2236, Dec. 2011.

XIAOLI LI received the B.E. and M.E. degrees from the Dalian University of Technology, in 1994 and 1997, respectively, and the Ph.D. degree from Northeastern University, China, in 2000. From 2000 to 2003, he was a Research Fellow with Tsinghua University, China, and with the Université Libre de Bruxelles, Belgium. He is currently a Professor with the Beijing University of Technology. His research interests include intelligent control, multiple model control, adaptive control, and robust control.

KANG WANG received the B.E. degree and Ph.D. degree in control science and engineering from the School of Automation and Electrical Engineering, University of Science and Technology Beijing, in 2012 and 2018, respectively. He is currently a Postdoctoral Researcher with the Faculty of Information Technology, Beijing University of Technology. His research interests include artificial neural networks, optimal control, and intelligent control.

CHAO JIA received the B.E. degree from the Qingdao University of Technology, in 2011, and the Ph.D. degree of control science and engineering from the University of Science and Technology Beijing, in 2017. He is currently an Engineer of China Electronics Standardization Institute. His research interests include neural networks, adaptive control, cyber-physical systems, and the industrial Internet.